

Article

Unveiling Non-Covalent Interactions in Novel Cooperative Photoredox Systems for Efficient Alkene Oxidation in Water

Isabel Guerrero ¹, Clara Viñas ¹ , Francesc Teixidor ^{1,*} and Isabel Romero ^{2,*} 

¹ Institut de Ciència de Materials de Barcelona (ICMAB-CSIC), Campus UAB, E-08193 Bellaterra, Spain; iguerrero@icmab.es (I.G.); clara@icmab.es (C.V.)

² Departament de Química and Serveis Tècnics de Recerca, Universitat de Girona, C/M. Aurèlia Campmany, 69, E-17003 Girona, Spain

* Correspondence: teixidor@icmab.es (F.T.); marisa.romero@udg.edu (I.R.)

Abstract: A new cooperative photoredox catalytic system, $[\text{Ru}^{\text{II}}(\text{trpy})(\text{bpy})(\text{H}_2\text{O})][3,3'\text{-Co}(8,9,12\text{-Cl}_3\text{-}1,2\text{-C}_2\text{B}_9\text{H}_8)_2]_2$, **5**, has been synthesized and fully characterized for the first time. In this system, the photoredox catalyst $[3,3'\text{-Co}(8,9,12\text{-Cl}_3\text{-}1,2\text{-C}_2\text{B}_9\text{H}_8)_2]^- [\text{Cl}_6\text{-}1]^-$, a metallocarborane, and the oxidation catalyst $[\text{Ru}^{\text{II}}(\text{trpy})(\text{bpy})(\text{H}_2\text{O})]^{2+}$, **2** are linked by non-covalent interactions. This compound, along with the one previously synthesized by us, $[\text{Ru}^{\text{II}}(\text{trpy})(\text{bpy})(\text{H}_2\text{O})][(3,3'\text{-Co}(1,2\text{-C}_2\text{B}_9\text{H}_{11}))_2]_2$, **4**, are the only examples of cooperative molecular photocatalysts in which the catalyst and photosensitizer are not linked by covalent bonds. Both cooperative systems have proven to be efficient photocatalysts for the oxidation of alkenes in water through Proton Coupled Electron Transfer processes (PCETs). Using 0.05 mol% of catalyst **4**, total conversion values were achieved after 15 min with moderate selectivity for the corresponding epoxides, which decreases with reaction time, along with the TON values. However, with 0.005 mol% of catalyst, the conversion values are lower, but the selectivity and TON values are higher. This occurs simultaneously with an increase in the amount of the corresponding diol for most of the substrates studied. Photocatalyst **4** acts as a photocatalyst in both the epoxidation of alkenes and their hydroxylation in aqueous medium. The hybrid system **5** shows generally higher conversion values at low loads compared to those obtained with **4** for most of the substrates studied. However, the selectivity values for the corresponding epoxides are lower even after 15 min of reaction. This is likely due to the enhanced oxidizing capacity of Co^{IV} in catalyst **5**, resulting from the presence of more electron-withdrawing substituents on the metallocarborane platform.

Keywords: photoredox alkene oxidation; metallocarborane; ruthenium; ion-pair cooperative catalysis; aqueous medium



Citation: Guerrero, I.; Viñas, C.; Teixidor, F.; Romero, I. Unveiling Non-Covalent Interactions in Novel Cooperative Photoredox Systems for Efficient Alkene Oxidation in Water. *Molecules* **2024**, *29*, 2378. <https://doi.org/10.3390/molecules29102378>

Academic Editors: Hai-yang Liu and Barbara Bonelli

Received: 24 April 2024

Revised: 13 May 2024

Accepted: 15 May 2024

Published: 18 May 2024



Copyright: © 2024 by the authors. Licensee MDPI, Basel, Switzerland. This article is an open access article distributed under the terms and conditions of the Creative Commons Attribution (CC BY) license (<https://creativecommons.org/licenses/by/4.0/>).

1. Introduction

Epoxides are an important and versatile part of intermediate and basic components that are used to obtain more elaborate chemical products in both organic synthesis and in the industrial production of fine and bulk chemical products [1,2]. For example, epoxides can be transformed into a variety of functionalized products as diols, aminoalcohols, allylic alcohols, ketones, etc. [3–6]. The chemical oxidation of alkenes to obtain the corresponding epoxides has been carried out using different metal catalysts such as Mn-salen catalyst and NaClO or variations of these [7,8], $\text{Ti}(\text{iPrO})_4$ [9,10], and Ru-aqua complexes [11,12], among others. Most of these processes have been studied in organic media.

The development of photocatalytic methods and systems for organic transformations is challenging given the significant environmental and economic impact that this entails [13]. Cooperative photoredox catalysis represents a significant advancement in this field. It involves two catalysts: one that is photochemically active and another that is redox active, even in the absence of light [14]. The redox-active metal complex serves as a catalyst to

activate either a water molecule or an organic substrate through a proton-coupled electron transfer (PCET) mechanism. Currently, photochemical systems studied for the oxidation of substrates involve a photocatalyst [15–17] or a photocatalyst combined with a transition metal catalyst based on polypyridyl compound [18–21]. However, a few examples of photochemical epoxidation of alkenes have been carried out with Earth-abundant metals [22–24]. Manganese and cobalt compounds all containing the carboranylcarboxylate ligand, $[1\text{-CH}_3\text{-2-CO}_2\text{-1,2-closo-C}_2\text{B}_{10}\text{H}_{10}]^-$, have been tested in the epoxidation of aliphatic and aromatic alkenes using peracetic acid as the oxidant [25]. The catalytic results highlight the role of the carboranylcarboxylate ligand in the selectivity of the processes, and it was found that coordination of the carboranylcarboxylate ligand to the metal ions is key to their catalytic performance.

On the other hand, it is well known that some boron clusters interact with light [26–28] and that they have been studied as catalysts in different processes. The most well-known metallocarborane is the anionic cobaltabis(dicarbollide) [29] that can be synthesized in high yield by a fast and environmentally friendly solid-state reaction [30]. The sandwich compound $\text{Na}[3,3'\text{-Co}(1,2\text{-C}_2\text{B}_9\text{H}_{11})_2]$, **Na [1]**, found by Fuentes et al. [31], has many possibilities to form hydrogen bonds (e.g., $\text{C}_c\text{-H}\cdots\text{O}$ or $\text{C}_c\text{-H}\cdots\text{X}$ (X = halogen) as well as dihydrogen bonding $\text{C}_c\text{-H}\cdots\text{H-B}$ and $\text{B-H}\cdots\text{H-N}$ (C_c stands for the cluster carbon atoms)) [32–34]. **Na [1]** is highly stable in water, but even at low concentrations it forms aggregates (vesicles and micelles) [35–37] and can form ion-pair complexes through hydrogen and dihydrogen interactions. These supramolecular interactions appear to be significant in electron transfer processes and therefore in the performance and efficiency of photocatalytic systems.

Recently, we have shown that **Na [1]** and its dichloro (**Na[Cl₂-1]**) and hexachloro (**Na[Cl₆-1]**), acting both as catalyst and photosensitizer, have been highly efficient in the photooxidation of alcohol [38] and **Na [1]** in the oxidation of alkenes [24] in water, through single electron transfer processes (SET). We have also supported the metallabis(dicarbollide) catalyst on silica-coated magnetite nanoparticles [39]. This system has proven to be a green and sustainable heterogeneous catalytic system, highly efficient, and easily reusable for the photooxidation of alcohols in water. Finally, we have synthesized a cooperative system where the cobaltabis(dicarbollide) was linked by non-covalent interactions to a redox active oxidation catalyst that represented an efficient photocatalyst for the photooxidation of alcohols in water through PCET [40]. This specific cooperative photocatalytic system has not yet been explored for the photooxidation of alkenes in an aqueous environment.

With all this in mind, we describe here the synthesis of a new ruthenium-cobaltabis (dicarbollide) compound, $[\text{Ru}^{\text{II}}(\text{terpy})(\text{bpy})(\text{H}_2\text{O})][3,3'\text{-Co}(8,9,12\text{-Cl}_3\text{-1,2-C}_2\text{B}_9\text{H}_8)_2]_2$ **5** (see Chart 1), where the $[\text{Ru-OH}_2]$ cation belongs to the family of redox oxidation catalysts [41] and the anion is the hexachloro cobaltabis(dicarbollide), $[3,3'\text{-Co}(8,9,12\text{-Cl}_3\text{-1,2-C}_2\text{B}_9\text{H}_8)_2]^-$, **[Cl₆-1]**[−]. Also, their complete spectroscopic and electrochemical characterization has been conducted. The photocatalytic behavior of **5**, together with that of the previously synthesized $[\text{Ru}^{\text{II}}(\text{terpy})(\text{bpy})(\text{H}_2\text{O})][3,3'\text{-Co}(1,2\text{-C}_2\text{B}_9\text{H}_{11})_2]_2$, **4**, as cooperative photoredox catalysts in the oxidation of aromatic and aliphatic alkenes in water has been tested and the results have been studied for the purpose of comparison.

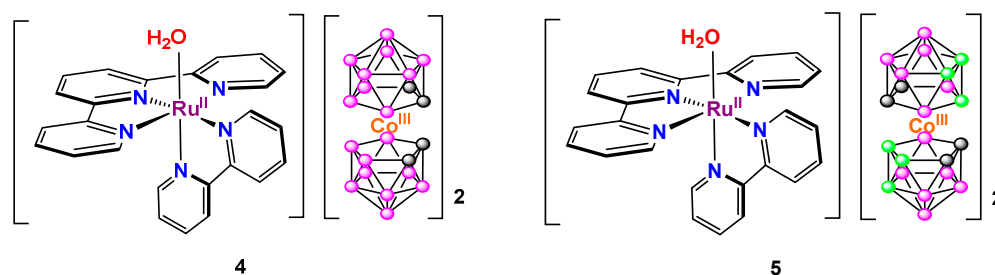
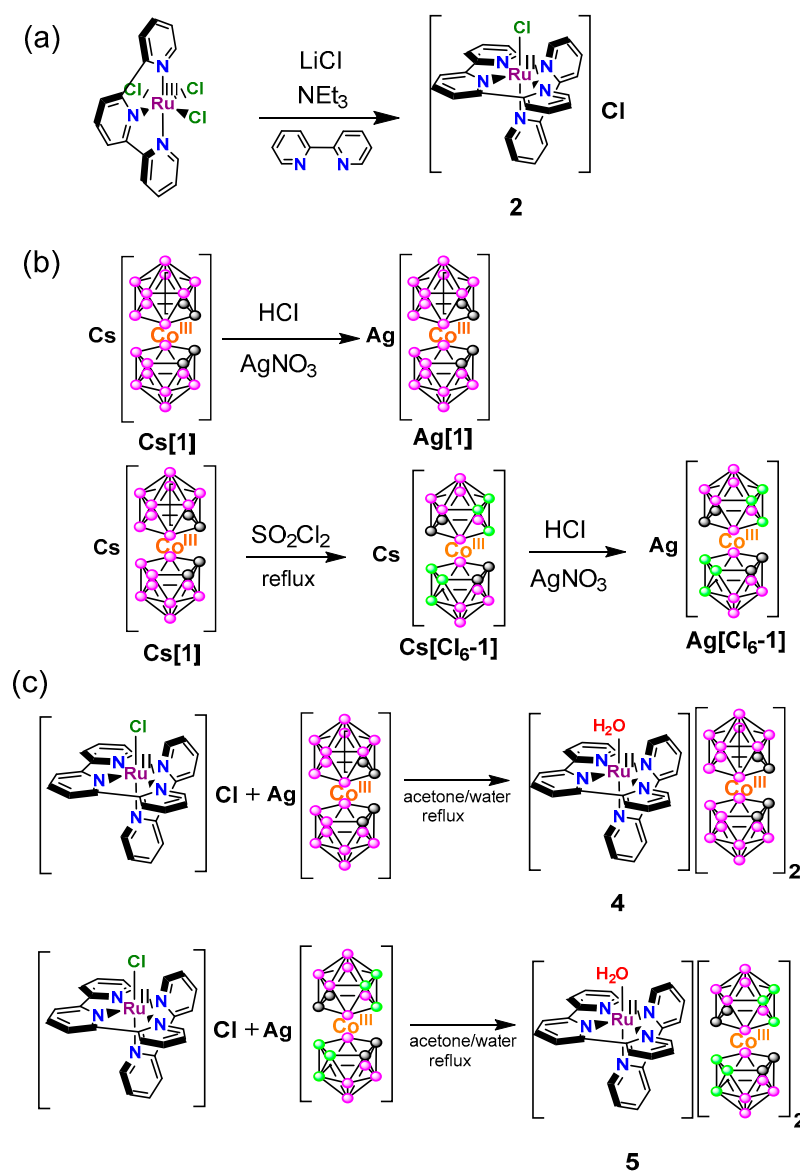


Chart 1. Schematic representation of ruthenium-cobaltabis(dicarbollide) complexes **4** (left) and **5** (right).

2. Results and Discussion

2.1. Synthesis, Spectroscopic, and Redox Characterization

The synthetic strategy followed for the preparation of the ruthenium-cobaltabis(dicarbollide) complex $[\text{Ru}^{\text{II}}(\text{terpy})(\text{bpy})(\text{H}_2\text{O})][(\text{3,3}'\text{-Co}(1,2\text{-C}_2\text{B}_9\text{H}_{11})_2)_2]$, **4** is described in [40,42] and the synthesis of $[\text{Ru}^{\text{II}}(\text{terpy})(\text{bpy})(\text{H}_2\text{O})][\text{3,3}'\text{-Co}(8,9,12\text{-Cl}_3\text{-1,2-C}_2\text{B}_9\text{H}_8)_2]$ **5** involves the preparation of $\text{Ag}[\text{Cl}_6\text{-1}]$, following the formation of $\text{H}[\text{Cl}_6\text{-1}]$ from the water insoluble **Cs [1]**. Then, cooperative system **5** is synthesized by dissolving $[\text{Ru}^{\text{II}}(\text{terpy})(\text{bpy})(\text{Cl})]\text{Cl}$, **2**, in a 1:1 mixture of water and acetone in the presence of $\text{Ag}[\text{Cl}_6\text{-1}]$ under reflux conditions, following the method described in [43]. After filtering out AgCl , a molecular aqua ruthenium (II) complex containing two hexachloro cobaltabis(dicarbollide) anions as counterions is isolated. The synthetic strategy is depicted in Scheme 1.



Scheme 1. Synthetic strategy for preparation of **4** and **5**. (a) Synthesis of **2** obtained following method described in [42]. (b) Synthesis of $\text{Ag}[\text{1}]$ following method described in [40] and $\text{Ag}[\text{Cl}_6\text{-1}]$. (c) Synthesis of compounds **4** and **5** by reaction between **2** and $\text{Ag}[\text{1}]$ and $\text{Ag}[\text{Cl}_6\text{-1}]$, respectively.

Figures 1, S1 and S2 display the IR spectra of complexes **4**, **5**, and $\text{Ag}[\text{Cl}_6\text{-1}]$. The IR of **4** and **5** show vibrations around 2900 and 3030 cm^{-1} that can be assigned to $\nu_{\text{C-H}}$ stretching modes for the aromatic rings of the cationic moieties and to the $\nu_{\text{C-H}}$ stretching

of the C-H bonds in the different rotamers of the dicarbollide anions, respectively. A band can be seen over 3500 cm^{-1} which corresponds to the $\nu_{\text{O-H}}$ stretching of the water ligands coordinated to ruthenium atoms in both compounds. We have also observed significant vibrations around 2530 cm^{-1} that correspond to $\nu_{\text{B-H}}$ stretching mode for the B-H bonds in the compounds. Unlike the spectrum of compound **4**, the spectra of compound **5** and **Ag[Cl₆-1]** presents bands at 900 cm^{-1} corresponding to $\nu_{\text{B-Cl}}$ stretching of the B-Cl bonds, present in the hexachloro cobaltabis(dicarbollide) anions.

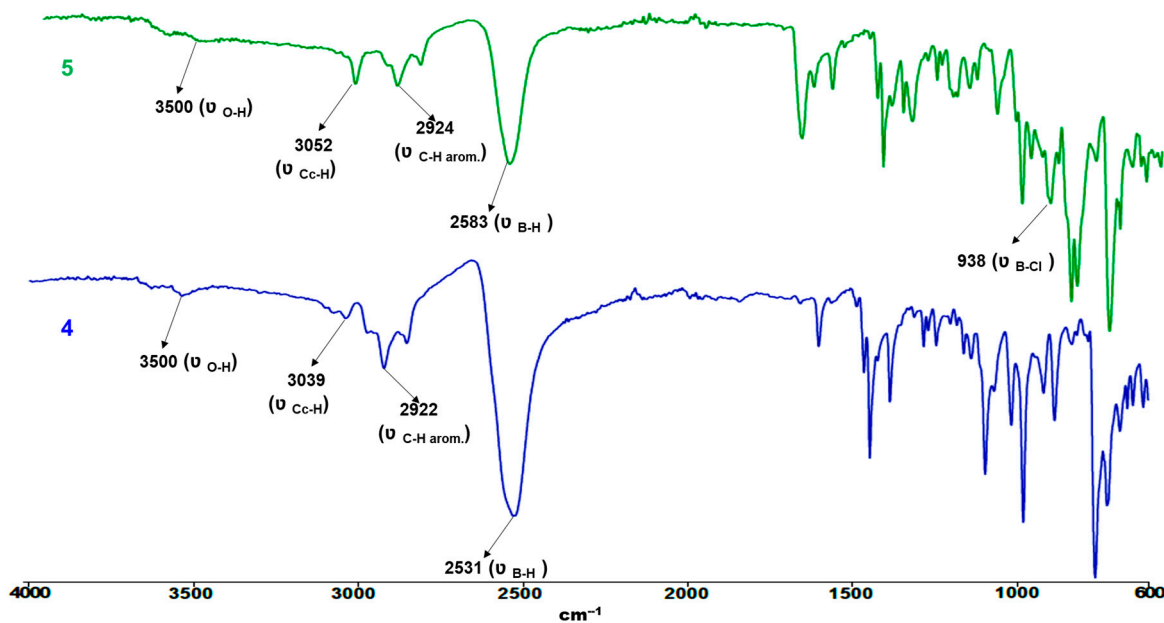


Figure 1. IR spectra of complexes **4** (blue) and **5** (green).

The 1D ^1H NMR spectra of the complex **Ag[Cl₆-1]** and compound **5**, along with the COSY spectrum of **5**, were recorded in acetone-*d*₆. These are displayed in Figures 2, S3 and S4, respectively. The ^1H NMR spectrum of **5** shows two set of signals, similar to complex **4** [40], (i) one in the aliphatic region that can be assigned to the C-H of the cobaltacarborane anions, which resonances appear around $\delta = 4.34$ ppm, showing a shift of 0.36 ppm to low field with respect to complex **4**; and (ii) the second one, in the aromatic region corresponding to the protons of the bipyridine and terpyridine ligands of the ruthenium cation.

The $^1\text{H}\{^{11}\text{B}\}$ NMR spectrum exhibits the H-B resonances over a wide range of chemical-shift in the region from $\delta = 1.70$ to 3.5 ppm (Figure S4b). The $^{11}\text{B}\{^1\text{H}\}$ NMR spectra displays signals corresponding to the non-equivalent boron atoms avoiding the B-H signals coupling. On the other hand, the ^{11}B NMR spectrum displays B-H signals as doublets and B-Cl signals as singlets. Both spectra show the typical pattern of the hexachloro cobaltabis(dicarbollide) cluster in the range from $\delta = 12.62$ to -24.38 ppm, as shown in Figure S4 [34].

The UV-vis spectrum of **Ag[Cl₆-1]** in CH_2Cl_2 shows one strong absorption band at 327 nm and three others with less intensity at 280, 390, and 469 nm, (Figure S5) in accordance with [43–45]. Figure 3 shows the UV-visible spectra of **5** and **2**. The former exhibits ligand-based π - π^* bands of the cationic part below 350 nm that are partially eclipsed by strong absorptions corresponding to the hexachloro cobaltabis(dicarbollide) anionic moiety. Above 350 nm, the spectra show less-intense bands that correspond to $d\pi(\text{Ru})-\pi^*(\text{L})$ MLCT transitions [46]. It is worth mentioning the shift to higher energy absorptions observed for the MLCT bands of **5** regarding those of complex **2**. This seems to indicate that the substitution of the chloride counterions by the metallacarboranes provokes the stabilization of the $d\pi$ (Ru) donor orbitals.

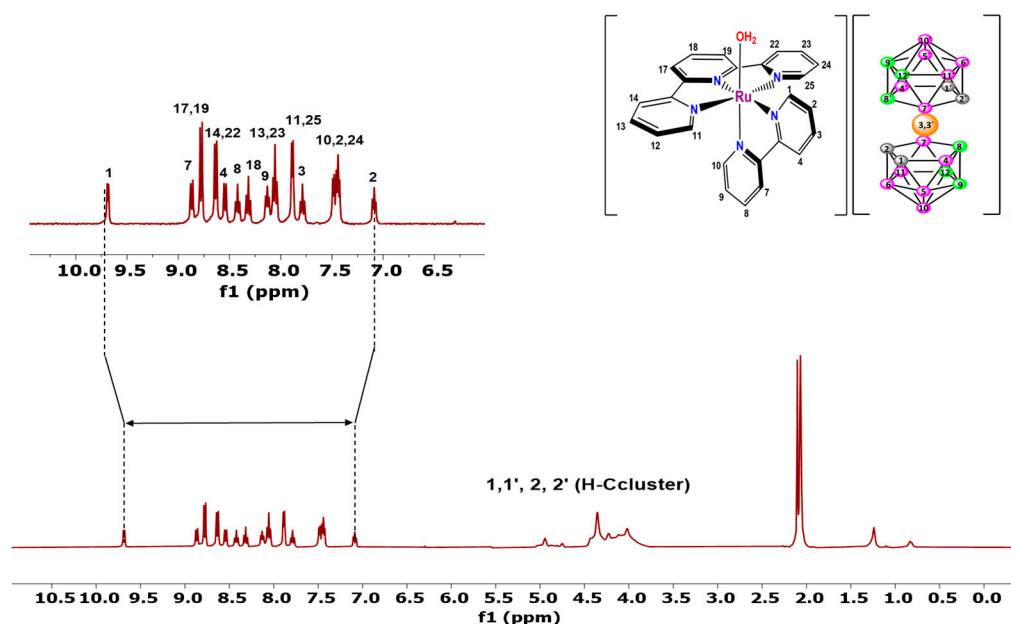


Figure 2. ^1H NMR spectrum of **5** in acetone- d_6 .

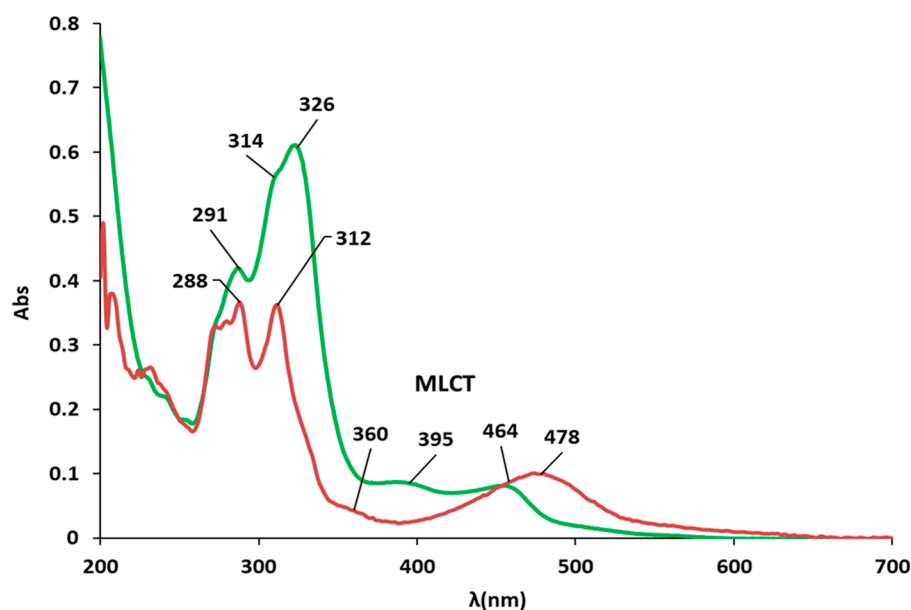


Figure 3. UV-vis spectrum of **5** (green line) and **2** (brown line) in dichloromethane.

The electrochemical behavior of complexes **Ag[Cl₆-1]** and **5** have been studied by means of cyclic voltammetry (CV). The CV curve of **Ag[Cl₆-1]** in $\text{CH}_3\text{CN} + 0.1 \text{ M } [n\text{-Bu}_4\text{N}][\text{PF}_6]$ (TBAH) shows one reversible one-electron-redox process at $E_{1/2} = -0.89 \text{ V}$ versus Ag/AgCl as reference electrode, which can be assigned to $\text{Co}^{\text{III}}/\text{Co}^{\text{II}}$ (see Figure S6). Unlike the derivative **Ag [1]**, the wave corresponding to $\text{Co}^{\text{IV}}/\text{Co}^{\text{III}}$ is not observed, probably because it is outside the working range of the solvent.

The CV of complex **5** in $\text{CH}_3\text{CN} + 0.1 \text{ M TBAH}$ exhibits different redox processes due to the ruthenium and cobalt ions. Two quasi-reversible monoelectronic $\text{Co}^{\text{III}} \text{Ru}^{\text{III}}/\text{Co}^{\text{III}} \text{Ru}^{\text{II}}$ and $\text{Co}^{\text{III}} \text{Ru}^{\text{IV}}/\text{Co}^{\text{III}} \text{Ru}^{\text{III}}$ redox waves at $E_{\text{pa}1} = 0.82 \text{ V}$; $E_{\text{pc}1} = 0.74 \text{ V}$ and $E_{\text{pa}2} = 1.17 \text{ V}$; $E_{\text{pc}2} = 0.93 \text{ V}$ vs. Ag/AgCl ($E_{\text{pa}1} = 0.38 \text{ V}$; $E_{\text{pc}1} = 0.31 \text{ V}$ and $E_{\text{pa}2} = 0.73 \text{ V}$; $E_{\text{pc}2} = 0.49$ vs. Fc^+/Fc) respectively and one quasireversible monoelectronic $\text{Co}^{\text{III}} \text{Ru}^{\text{II}}/\text{Co}^{\text{II}} \text{Ru}^{\text{II}}$ redox wave at $E_{\text{pa}3} = -0.76 \text{ V}$; $E_{\text{pc}3} = -0.97 \text{ V}$ vs. Ag/AgCl , ($E_{\text{pa}3} = -1.19 \text{ V}$; $E_{\text{pc}3} = -1.40 \text{ V}$ vs. Fc^+/Fc) (Figure S6). The redox wave corresponding to the $\text{Co}^{\text{IV}} \text{Ru}^{\text{IV}}/\text{Co}^{\text{III}} \text{Ru}^{\text{IV}}$ is

not observed. The two successive one-electron oxidation waves that correspond to $\text{Co}^{\text{III}}\text{Ru}^{\text{III}}/\text{Co}^{\text{III}}\text{Ru}^{\text{II}}$ and $\text{Co}^{\text{III}}\text{Ru}^{\text{IV}}/\text{Co}^{\text{III}}\text{Ru}^{\text{III}}$ redox couples can be assigned to two PCETs as it was observed in complex **4** [40]. These values have been assigned to the $\text{Ru}^{\text{III}}/\text{Ru}^{\text{II}}$ and $\text{Ru}^{\text{IV}}/\text{Ru}^{\text{III}}$ couples of the catalytic unit based in the values presented by the mononuclear $[\text{Ru}^{\text{II}}(\text{terpy})(\text{bpy})(\text{H}_2\text{O})]^{2+}$ compound, [42,47] and in accordance with the values observed in complex **4**. This last compound, unlike **5**, shows one more oxidation wave attributed to $\text{Co}^{\text{IV}}\text{Ru}^{\text{IV}}/\text{Co}^{\text{III}}\text{Ru}^{\text{IV}}$ redox couple a $E_{1/2} = 1.38$ vs. Ag/AgCl (0.95 V vs. Fc^+/Fc). In **5**, this potential would likely be outside the working range due to the greater oxidizing character of the anion $[\text{Cl}_6\text{-1}]^-$ compared to $[\text{1}]^-$.

As has been observed with **4** in water [42], it is expected that in both compounds **4** and **5** the photogenerated Co^{IV} could oxidize $[\text{Ru}^{\text{III}}\text{-OH}]^{2+}$ to $[\text{Ru}^{\text{IV}}\text{=O}]^{2+}$, since the potential for $\text{Co}^{\text{IV}}/\text{Co}^{\text{III}}$ is high enough compared to the $\text{Ru}^{\text{IV}}/\text{Ru}^{\text{III}}$ couple. Then, it is expected that for photocatalytic oxidation of alkenes, both $[\text{1}]^-$ and $[\text{Cl}_6\text{-1}]^-$ could act as good photosensitizers.

2.2. Photocatalytic Alkene Oxidations

The photocatalysts **4** and **5** are $[\text{Ru}][\text{Co}]_2$ ion pairs based on Co, an abundant transition metal, whereas the redox parts are Ru-OH₂ complexes. The first photocatalytic alkene oxidation experiments were all performed using **4** as the photocatalyst by exposing the reaction quartz vials to UV irradiation (2.2 W, $\lambda \sim 300$ nm) at room temperature and atmospheric pressure using styrene as substrate and very relevantly using water as a solvent. The samples were made of 5 mL of water pH = 7 (K_2CO_3 solution is used to adjust the pH) with a mixture of **4** (0.01 mM), styrene (20 mM), and $\text{Na}_2\text{S}_2\text{O}_8$ (26 mM) as oxidizing agent, (catalyst load of 0.05 mol%). Then, different reaction times were tested to assess the conversion as a function of time. The reaction products were extracted with dichloromethane six times, dried with Na_2SO_4 and quantified by means of GC-MS analysis. As can be observed in Figure S7, after 30 min of reaction, even after 15 min, all the styrene was converted. Blank experiments after 30 min of reaction, in the absence of catalyst, light, or oxidizing agent, showed that no significant conversion of styrene occurred. Figure 4 displays (a) the yields of different oxidation products obtained at different times and (b) the molar fractions (X_M) obtained in function of the reaction time. As we can see, after 5 min the amount of epoxide obtained is high (67%) and after 15 min the amount of diol increases, although the amount of epoxide is still greater (35% diol vs. 57% epoxide). A slight decrease in epoxide is observed after 30 min, (34% diol vs. 51% epoxide), but in any case, it continues to be the majority product above diol and other byproducts such as benzaldehyde and benzoic acid. We observed a slight decrease in yield and selectivity for epoxide formation with longer reaction times. Therefore, we selected a 15-min reaction time for the photoredox oxidation of various alkenes. However, we also examined the catalyst's performance after a 30-min reaction in some instances.

Table 1 displays the performance of the photocatalyst **4** after 5, 15, and 30 min of reaction using 0.05 mol% and 0.005 mol% of catalyst. In general, when 0.05 mol% of catalyst is used, it can be observed that total conversion values were achieved after 15 min of reaction with, in many cases, total conversion after 30 min. However, moderate selectivity in the corresponding epoxide is obtained, which decreases when the reaction time increase, along with the TON values. However, with 0.005 mol% of catalyst the conversion values after 15 and 30 min are lower but the selectivity and TON values are higher. This happens simultaneously with an increase in the amount of the corresponding diol for most of the substrates studied (see Table S1). At this point we can assert that the selectivity towards the epoxide increases with lower loads of catalyst **4**.

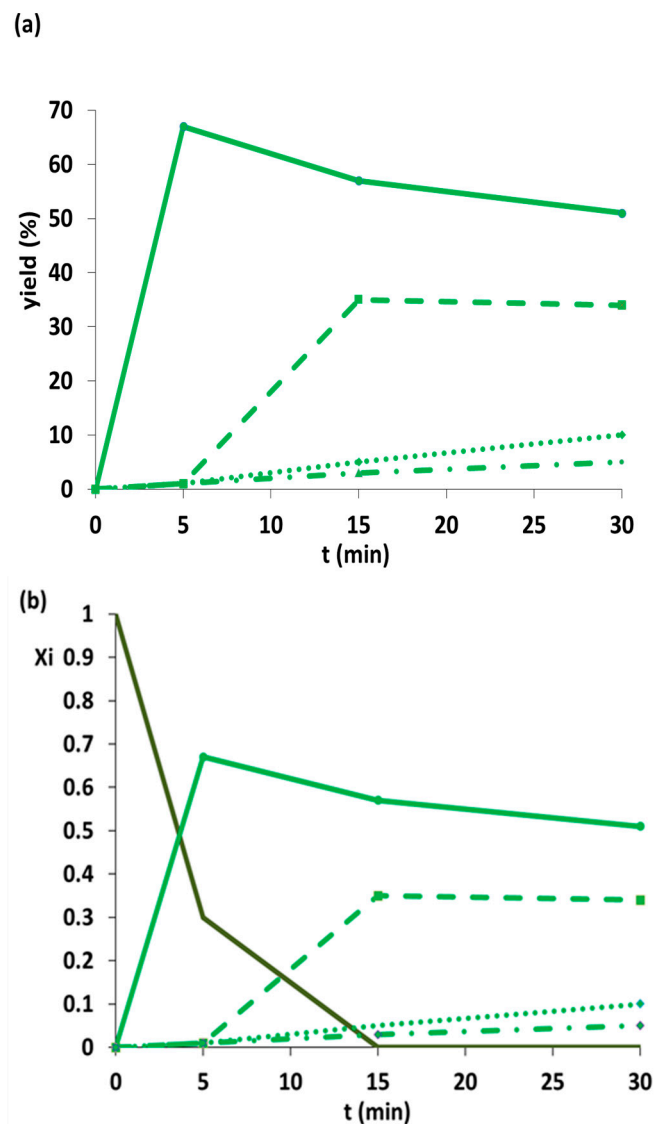


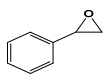
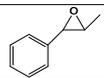
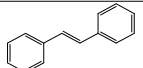
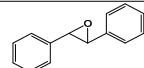
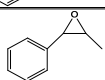
Figure 4. (a) Plot of yield as function of time and (b) plot of molar fractions (X_M) as function of time for photoredox catalysis of styrene. Dark green line: styrene; green line: styrene oxide; dashed line: 1-phenyl-1,2-ethanediol; dash dotted line: benzaldehyde; dotted line: benzoic acid. Conditions: $[\text{Ru}^{\text{II}}(\text{terpy})(\text{bpy})(\text{H}_2\text{O})][(\text{3,3}'\text{-Co}(1,2\text{-C}_2\text{B}_9\text{H}_{11})_2)_2]$ (0.01 mM), styrene (20 mM), $\text{Na}_2\text{S}_2\text{O}_8$ (26 mM), 5 mL aqueous solution at pH = 7, light irradiation (2.2 W, $\lambda \sim 300$ nm).

The photoepoxidation of *trans*- β -methylstyrene (entry 2), *trans*-stilbene (entry 3) led to the formation of the corresponding *trans*-isomer without isomerization after 15 and 30 min; however, in the case of *cis*- β -methylstyrene, the stereoselectivity towards the formation of the *cis*-epoxide isomer decreases after 30 min of reaction. The oxidation of aliphatic alkenes as the cyclic cyclooctene (entry 5) together with linear 1-octene (entry 6) has also been tested. In both cases, a good performance is shown.

As we have commented previously, the selectivity towards the epoxide in water decreased with the reaction time whereas the amount of diol increases as well as, in some cases, other overoxidation products. In an aqueous medium, the epoxide ring undergoes ring opening. However, we aimed to determine whether this process is driven by water or by our catalyst. Different experiments were then performed by exposing the sealed reaction to UV irradiation for 15 and 30 min, operating with 0.05 mol% of catalyst, under the same conditions used before and using three different epoxides: 1,2-epoxyoctane, styrene oxide, and *trans*-stilbene oxide. The results shown in Table S2 indicate the formation of the

corresponding diols in water after 15 and 30 min if the photocatalyst is present. When the catalyst is absent, lower or nonexistent yields of diols have been observed. In the case of styrene, only benzaldehyde or benzoic acid has been detected after 30 min. Thus, we can conclude that **4** acts as a photocatalyst in both processes, epoxidation, and hydroxylation in aqueous media. It is worth mentioning that ring opening of epoxides is a promising process to produce 1,2-diols, an important functional group to produce pharmaceuticals, surfactants, or their intermediates [48].

Table 1. Photooxidation tests performed with ruthenium cobaltabis(dicarbollide) complex **4**.

Entry	Substrate	Conv.(selec.)%		Product	TON	
		0.05 mol%	0.005 mol%		0.05 mol%	0.005 mol%
1		70(96) [a]			1344 [a]	
		≥99(57) [b]	73(56) [b]		1140 [b]	8200 [b]
		≥99(51) [c]	≥99(61) [c]		1020 [c]	12,200 [c]
2		96(79) [b]			1520 [b]	
		≥99(69) [c]	91(≥99) [c]		1380 [c]	18,200 [c]
3		89(96) [b]	80(≥99) [b]		1700 [b]	16,000 [b]
		97(54) [c]	≥99(71) [c]		1040 [c]	14,200 [c]
4		≥99(91) [b]	61(≥99) [b]		1820 (59%,cis) [b]	12,200 (46%,cis) [b]
		≥99(60) [c]	73(≥99) [c]		1200 (36%,cis) [c]	14,600 (27%,cis) [c]
5		≥99(67) [b]	68(66) [b]		1340 [b]	9000 [b]
		≥99(55) [c]	85(41) [c]		1100 [c]	6970 [c]
6		≥99(69) [b]	58(≥99) [b]		1380 [b]	11,600 [b]
		≥99(35) [c]	95(≥99) [c]		700 [c]	19,000 [c]

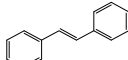
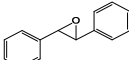
Conditions: **4** (0.01 or 0.001 mM), substrate (20 mM), Na₂S₂O₈ (26 mM), 5 mL aqueous solution at pH = 7. [a] 5 min of reaction, [b] 15 min and [c] 30 min of reaction.

We have also studied the behavior of **5** as photocatalyst in the alkene oxidation in water using low catalyst load of 0.005 mol%. The results are presented in Tables 2 and S3, including those previously obtained for compound **4**, to facilitate a comparative analysis. In general, we can observe moderate-to-high conversion values after 30 min of reaction in most cases. It is worth noting that while the conversion values of catalyst **5** are generally higher than those obtained with **4**, in most of the substrates studied, the selectivity values in the corresponding epoxides are lower even after 15 min of reaction. This is probably due to the enhanced oxidizing capacity of Co^{IV} in catalyst **5**, as a consequence of the presence of more electron-withdrawing substituents on the cosane platform. At this point, we can assert that in most cases and under the studied conditions, photocatalyst **4** shows higher selectivity values towards the epoxidation of alkenes than photocatalyst **5**.

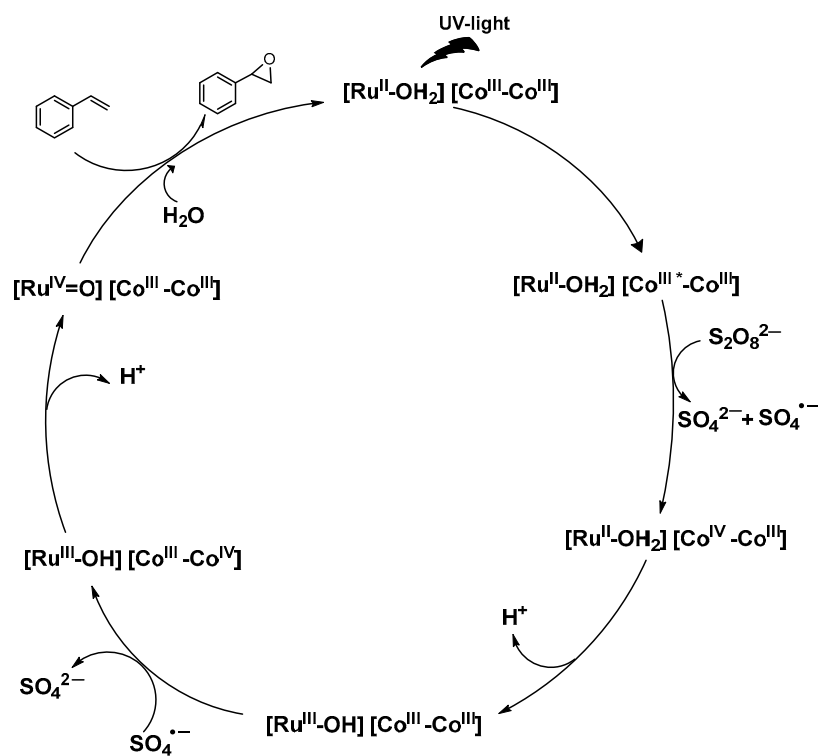
Based on the photocatalytic results exposed above, we have postulated a mechanism, displayed in Figure 5, for the photoepoxidation of alkenes carried out by complexes **4** and **5**.

In the mechanism that is consistent with the products generated, the absorption of light by the photosensitizer Co_p^{III} produces the excitation to form Co_p^{III*}, which undergoes oxidative quenching by S₂O₈²⁻ (oxidizing agent) generating Co_p^{IV}. This photogenerated strong oxidizing Co^{IV} can oxidize Ru_c^{II}-OH₂ to Ru_c^{III}-OH. Then, the SO₄⁻ radical oxidizes a new Co_p^{III} to Co_p^{IV} which oxidizes Ru_c^{III}-OH to Ru_c^{IV}=O species. The Ru_c^{IV}=O species reacts with the corresponding alkene to afford the oxidized products, with the regeneration of the corresponding catalyst Ru_c^{II}-OH₂. With the pathway proposed in Figure 5, the exchange of two electrons and two protons takes place in the oxidation of alkenes.

Table 2. Photooxidation tests performed with ruthenium cobaltabis(dicarbollide) complexes 4 and 5.

Entry	Substrate	Conv.(selec.)%		Product	TON	
		4	5		4	5
1		73(56) ^[a] ≥99(61) ^[b]	75(31) ^[a]		8200 ^[a] 12,200 ^[b]	4600 ^[a]
2		91(≥99) ^[b]	87(≥99) ^[b]		18,200 ^[b]	17,400 ^[b]
3		80(≥99) ^[a] ≥99(71) ^[b]	≥99(86) ^[a] ≥99(83) ^[b]		16,000 ^[a] 14,200 ^[b]	17,200 ^[a] 16,600 ^[b]
4		61(≥99) ^[a] 73(≥99) ^[b]	88(57) ^[a] 89(57) ^[b]		12,200 (46%,cis) ^[a] 14,600 (73%,trans) ^[b]	10,000 (50%,trans) ^[a] 10,100 (51%,trans) ^[b]
5		68(66) ^[a] 85(41) ^[b]	92(≥99) ^[a] 96(55) ^[b]		9000 ^[a] 6970 ^[b]	18,400 ^[a] 10,600 ^[b]

Conditions: 4 or 5 (0.001 mM), substrate (20 mM), Na₂S₂O₈ (26 mM), 5 mL aqueous solution at pH = 7. Ratio 1:2000:2600 or 1:20,000:26,000, ^[a] 15 min of reaction, ^[b] 30 min of reaction.

**Figure 5.** Proposed mechanism for alkene photooxidation.

3. Experimental

3.1. Materials, Instrumentation, and Measurements

The commercial Cs[Co(1,2-C₂B₉H₁₁)₂], Cs [1], was obtained of Katchem Spol.sr.o. Compounds [Ru^{III}Cl₃(terpy)], [49], [Ru^{II}Cl(terpy)(bpy)]Cl, 2, [Ru^{II}(terpy)(bpy)(OH)₂](ClO₄)₂, 3 [42,47] and [Ru^{II}(terpy)(bpy)(H₂O)][(3,3'-Co(1,2-C₂B₉H₁₁)₂)₂], 4 [40] were also prepared according to literature procedures. All synthetic manipulations were performed under nitrogen atmosphere using vacuum line techniques.

All reagents used in the present work were obtained from Aldrich Chemical Co. and were used without further purification. Reagent grade organic solvents were obtained from

SDS, and high purity deionized water was obtained by passing distilled water through a nano-pure Mili-Q water purification system.

UV-vis spectroscopy was performed on a Cary 50 Scan Varian (Santa Clara, CA, USA) UV-vis spectrophotometer with 1 cm quartz cells or with an immersion probe of 5 mm path length. NMR spectra have been recorded with a Bruker ARX 300 instrument (Bruker Biospin, Rheinstetten, Germany) and ^1H NMR spectra were recorded in acetone- d_6 . Chemical shift values were referenced to SiMe_4 . Elemental analyses were performed using a CHNS-O Elemental Analyser EA-1108 from Fisons (Waltham, USA). ESI-MS experiments were performed on a Navigator LC/MS chromatograph from Thermo Quest Finnigan (Toronto, Canada) using acetonitrile as mobile phase. Cyclic voltammetric (CV) or differential pulse voltammetry (DPV) was performed in an IJ-Cambria 660C potentiostat using a three-electrode cell. Glassy carbon electrode (3 mm diameter) from BAS was used as working electrode, platinum wire as auxiliary, and Ag as pseudo-reference electrode or SCE as the reference electrode. All cyclic voltammograms presented in this work were recorded under nitrogen atmosphere. The complexes were dissolved in deoxygenated solvents containing the necessary amount of TBAH as supporting electrolyte to yield a 0.1 M ionic strength solution. All $E_{1/2}$ values reported in this work were estimated from cyclic voltammetry experiments as the average of the oxidative and reductive peak potentials ($E_{\text{pa}} + E_{\text{pc}}$)/2. Unless explicitly mentioned, the concentration of the complexes was approximately 1 mM.

Gas chromatography was performed with a GC-2010 Gas Chromatograph from Shimadzu (Kyoto, Japan), equipped with an Astec CHIRALDEX G-TA column, 30 m \times 0.25 mm (i.d); FID detector, 250 $^\circ\text{C}$; injection: 250 $^\circ\text{C}$; carrier gas: helium; rate: 1.57 mL min^{-1} ; area normalization. The product analyses in the catalytic experiments were performed by GC with biphenyl as internal standard.

3.2. Synthesis of Compounds

Synthesis of Ag [3,3'-Co(8,9,12-Cl₃-1,2-C₂B₉H₈)₂], **Ag[Cl₆-1]**. A sample of Cs [3,3'-Co(1,2-C₂B₉H₁₁)₂], **Cs [1]** (0.45 g, 0.985 mmol) was dissolved in 14 mL of acetonitrile under magnetic stirring. It was then slowly added dropwise 14 mL of SO₂Cl₂ and the reaction mixture was refluxed 2 h at 70 $^\circ\text{C}$. Afterwards, volatiles were removed in the rotavapor and the resulting residue was extracted three times with diethyl ether (15 mL) and aqueous HCl (3M, 3 \times 15 mL) to remove all impurities. Then, the organic layer was dried over MgSO₄. After filtration, the liquid was evaporated and dissolved in water and precipitated using a saturated aqueous solution of CsCl. An orange solid was isolated. Then, the solvent was evaporated and the remaining solid was dissolved in 20 mL of diethylether. Further purification was performed by extraction procedure by hydrochloric acid 1M (3 \times 15 mL). The organic phase containing H [3,3'-Co(8,9,12-Cl₃-1,2-C₂B₉H₈)₂] (**H[Cl₆-1]**), was carried out to dryness under reduced pressure and dissolved with water. It was then added to an excess of silver nitrate (0.251 g, 1.477 mmol) to form a precipitate that was collected on a frit and washed with water three times and dried under vacuum. Yield 371.0 mg (60%). MALDI-TOF-MS: m/z calc. for [Cl₆-1]⁻: 530.40; m/z found (%): 495.95 [Cl₅-1] (8%), 529.91 [Cl₆-1] (85.02%), 563.86 [Cl₇-1] (7%). IR (ν , cm^{-1}): 3049 (wk, C-H), 2600 (shp, B-H), 1605 (O-H), 993 (B-Cl). ^1H [^{11}B] NMR (400 MHz, CD₃OCD₃): δ 4.35 (br s, 4H, C-H), 3.51, 3.34, 3.08, 2.91, 2.32, 1.69 (br s, 12H, B-H). ^{11}B NMR (96.29 MHz, CD₃OCD₃): δ = 12.14 (m, 2B, B-H, B8, B8'), 4.60 (m, 6B, B-H, B9, B9', B12, B12', B7, B7'), -5.24 (m, 4B, B-H, B10, B10', B4, B4'), -17.90 (d, 1J(B,H) = 156 Hz, 4B, B-H, B5, B5', B11, B11'), -24.38 (d, 1J(B,H) = 162 Hz, 2B, B-H, B6, B6'). $E_{1/2}$ Co^{III/II}(CH₃CN + 0.1M TBAH): -0.89 V vs. Ag. UV-vis (CH₃CN, 1 \times 10⁻⁴ M): λ_{max} nm (ϵ , M⁻¹ cm⁻¹) 240 (2978), 281 (7264), 328 (29,289), 391 (4014), 472 (484).

Synthesis of [Ru^{II}(terpy)(bpy)(H₂O)][3,3'-Co(8,9,12-Cl₃-1,2-C₂B₉H₈)₂], **5**. A sample of 0.09 g (0.142 mmol) of **2** and (0.26 g, 0.401 mmol) sample of **Ag[Cl₆-1]** were dissolved in 60 mL of acetone:water (1:1) and the resulting solution was refluxed for 3 h. Then, AgCl was filtered off through a frit containing celite. The volume of the solution was reduced and the mixture chilled in a refrigerator for 48 h. The orange precipitate was collected on

a frit, washed with cold water and anhydrous ethylether, and then vacuum-dried. Yield: 0.261 g (42%). Anal. Found (Calc.) for $C_{33}H_{53}B_3Cl_{12}Co_2N_5ORu \cdot 0.77H_2O \cdot 2Et_2O$: C, 28.52 (28.52); H, 3.71 (4.35); N, 3.90 (4.03) %. 1H NMR (acetone- d_6 , 400 MHz): δ 9.87 (d, 1H, $^3J_{H-H} = 5.6$ Hz, 1H, H1), 8.97 (d, 1H, $^3J_{H-H} = 8.0$ Hz, 1H, H7), 8.91 (d, $^3J_{H-H} = 7.9$ Hz, 2H, H17, H19), 8.77 (d, $^3J_{H-H} = 8.2$ Hz, 2H, H14, H22), 8.65 (d, $^3J_{H-H} = 8.1$ Hz, 1H, H4), 8.57 (td, $^3J_{H-H} = 8.1$ Hz, $^4J_{H-H} = 1.2$ Hz, 1H, H8), 8.48 (t, $^3J_{H-H} = 8.3$ Hz, 1H, H18), 8.19 (ddd, $^3J_{H-H} = 7.1$ Hz, $^4J_{H-H} = 1.0$ Hz, 1H, H9), 8.13 (td, $^3J_{H-H} = 7.9$ Hz, $^4J_{H-H} = 1.2$ Hz, 2H, H13, H23), 8.05 (d, $^3J_{H-H} = 5.4$ Hz, 2H, H11, H25), 7.89 (td, $^3J_{H-H} = 8.4$ Hz, $^4J_{H-H} = 1.3$ Hz 1H, H3), 7.65 (m, 3H, H10, H12, H24), 7.57 (td, $^3J_{H-H} = 8.0$ Hz, $^4J_{H-H} = 1.3$ Hz, 1H, H2), 5.83 (s, 2H, Ru-OH₂), 4.34 (s, 8H, C_c-H). $^1H\{^{11}B\}$ NMR (acetone- d_6 , 400 MHz): δ 4.34 (s, 8H, C_c-H), 3.07 (s, 8B-H, B4, B4', B7, B7'), 2.89 (s, 4B-H, B10, B10'), 1.97 (s, 4B-H, B6, B6'), 1.91 (s, 4B-H, B5, B5'), 1.67 (s, 4B-H, B11, B11'). ^{11}B NMR (acetone- d_6 , 128 MHz): δ 12.59 (d, 4B, $J_{B-H} = 116.6$ Hz, B-Cl), 4.82 (m, 8B, B-Cl), 1.99 (m, 4B, B-H), -5.17 (d, 4B, $J_{B-H} = 164.9$ Hz, B-H), -17.94 (d, 8B, $J_{B-H} = 162.5$ Hz, B-H), -24.41 (d, 4B, $J_{B-H} = 177.9$ Hz, B-H). $^{11}B\{^1H\}$ NMR (acetone- d_6 , 128 MHz): δ 12.62 (brs, 4B, B8, B8'), 4.82 (s, 8B, B9, B9', B12, B12'), 2.82 (s, 4B, B7, B7'), -5.05 (s, 4B, B10, B10'), -17.88 (s, 8B, B5, B5', B11, B11'). $^{13}C\{^1H\}$ -NMR (acetone- d_6 , 100 MHz): δ 159.30, 159.14, 158.65, 156.02, 153.12, 152.74, 150.53, 138.45, 137.53, 136.19, 136.05, 127.96, 127.59, 126.46, 124.18, 124.12, 123.59 and 123.28, (C **terpy-Ru-bpy**) and 47.42 (C_c). E_{1/2} (CH₂Cl₂+0.1 M TBAH) Co^{III/II}, -0.87 V; Co^{IV/III}, 1.39; Ru^{III/II}, 0.67 V; Ru^{IV/III}, 0.97 V vs. Ag. IR (ν_{max} , cm⁻¹): 3052, 2924, 2853, 2583, 1694, 1602, 1446, 1465, 1447, 1386, 1100, 1025, 938, 858, 875, 760. UV-vis (CH₃CN, 1×10^{-5} M) [λ_{max} nm (ϵ , cm⁻¹ M⁻¹): 232 (24,156), 244 (21,064), 291 (40,756), 314 (57,401), 326 (60,042), 395 (8855), 464 (7124)]. MS (ESI⁺) in acetonitrile (m/z): 1591.3 [M + K]⁺, 1021.20 [M-[Cl₆-1]⁻]⁺, 530.1 [Cl₆-1]⁻.

3.3. Photocatalytic Studies

A quartz tube containing an aqueous solution (5 mL) at pH 7 (K₂CO₃ solution is used to adjust the pH) with **4** or **5**, as catalysts, alkene as substrate, and Na₂S₂O₈ as sacrificial acceptor was exposed to UV light (2.2 W, $\lambda = 300$ nm or 352 nm) for different times. The complex: substrate: sacrificial oxidant ratios used (1:2000:2600 and 1:20,000:26,000 corresponding to concentrations of 0.01:20:26 mM and 0.001:20:26 mM, respectively). The concentrations were varied according to the study. For each experiment, a light reactor supplied light illumination with 12 lamps that produce UVA light at room temperature. The resulting solutions were extracted with CH₂Cl₂ six times. The solution was dried with anhydrous sodium sulfate and the solvent was reduced to a minimum volume under reduced pressure, then 100 μ L of biphenyl 100 mM as internal standard was added to the resulting solution, 2 mM in the resulting 5 mL solution. To check the reproducibility of the reactions, all the experiments were performed in triplicate and analyzed by Gas Chromatography.

3.4. Gas Chromatography Studies

Studies were performed with a GC-2010 Gas Chromatograph from Shimadzu, equipped with an Astec CHIRALDEX G-TA column, 30 m \times 0.25 mm (i.d) (Fukuoka, Japan); FID detector, 250 $^{\circ}$ C; injection: 250 $^{\circ}$ C; carrier gas: helium; rate: 1.57 mL/min; area normalization. For alkenes, substrates and products of catalysis were detected under the following conditions: styrene and derivatives: column temperature, 80 $^{\circ}$ C for 5 min, raising to 170 $^{\circ}$ C in a rate of 10 $^{\circ}$ C/min, holding 170 $^{\circ}$ C for 6 min. Trans- β -methyl-styrene, cis- β -methyl-styrene, cis-cyclooctene and derivatives: column temperature, 40 $^{\circ}$ C for 5 min, raising to 170 $^{\circ}$ C in a rate of 5 $^{\circ}$ C/min, holding 170 $^{\circ}$ C for 2 min. 1-octene and derivatives: column temperature, 30 $^{\circ}$ C for 5 min, raising to 170 $^{\circ}$ C in a rate of 10 $^{\circ}$ C/min, holding 170 $^{\circ}$ C for 3 min. Trans-stilbene and derivatives: column temperature, 50 $^{\circ}$ C for 1 min, raising to 150 $^{\circ}$ C in a rate of 15 $^{\circ}$ C/min, holding 150 $^{\circ}$ C for 2 min, then raising to 170 $^{\circ}$ C in a rate of 4 $^{\circ}$ C/min, holding 170 $^{\circ}$ C for 12 min. The product analyses in the catalytic experiments were performed by GC with biphenyl as internal standard.

4. Conclusions

Two cooperative ion pair photoredox systems $[\text{Ru}^{\text{II}}(\text{terpy})(\text{bpy})(\text{H}_2\text{O})][(\text{3,3}'\text{-Co(1,2-C}_2\text{B}_9\text{H}_{11})_2)_2]$, **4** and $[\text{Ru}^{\text{II}}(\text{terpy})(\text{bpy})(\text{H}_2\text{O})][\text{3,3}'\text{-Co(8,9,12-Cl}_3\text{-1,2--C}_2\text{B}_9\text{H}_8)_2]$ **5** have been studied as photoredox catalysts in the oxidation of aromatic and aliphatic alkenes in water. Both systems are formed by the same aqua ruthenium complex, $[\text{Ru}^{\text{II}}(\text{terpy})(\text{bpy})(\text{OH}_2)]^{2+}$, as electron transfer agent and by cobaltabis(dicarbollides), as light collectors; in **4** by $[\text{3,3}'\text{-Co-(1,2-C}_2\text{B}_9\text{H}_{11})_2]^-$ [**1**][−] and in **5** by $[\text{3,3}'\text{-Co(8,9,12-Cl}_3\text{-1,2--C}_2\text{B}_9\text{H}_8)_2]^-$ [**Cl}_6\text{-1}**][−]. Both the cobaltabis(dicarbollide) and the ruthenium aqua complex are linked by non-covalent interactions, avoiding costly covalent bonding. Complex **4** was previously synthesized by us and **5** has been easily made by the reaction of the chlorido Ru(II) complex, with **Ag[Cl}_6\text{-1}** in water/acetone (1:1) under reflux. The electrochemical studies evidence that the photogenerated Co^{IV} can easily oxidize $[\text{Ru}^{\text{III}}\text{-OH}]^{2+}$ to $[\text{Ru}^{\text{IV}}\text{=O}]^{2+}$ in water via PCETs as we have evidenced in the photocatalytic oxidation of alkenes in water.

We have highlighted the capacity of **4** to perform as excellent cooperative photoredox catalyst in the oxidation of alkenes in water using catalyst loads of 0.05 and 0.005 mol%, achieving high yields even when short reaction times of irradiation have been used. Using 0.05 mol% of catalyst, the epoxidation of styrene led to a slight decrease in epoxide after 30 min, but in any case, it continues to be the majority product above diol and other byproducts such as benzaldehyde and benzoic acid. For the rest of the substrates studied, the selectivity of epoxide decreases after 30 min. With 0.005 mol% of photocatalyst, the conversion values after 15 and 30 min are lower but the selectivity for the corresponding epoxide and TON values are higher. Compound **4** serves as a photocatalyst for both epoxidation and hydroxylation processes in aqueous media. When using catalyst **5** with a 0.005 mol% loading, the conversion values are typically higher than those achieved with compound **4**. However, in most cases, the selectivity towards the corresponding epoxides is lower, even after a 15-min reaction period. This difference is likely attributed to the enhanced oxidizing capacity of Co^{IV} in catalyst **5**.

To our knowledge, these are the first examples of cooperative systems featuring robust non-bonding interactions, which omit covalent bonds and have not previously been explored as photoredox catalysts for the epoxidation of alkenes in water. We have proposed a potential mechanism.

Supplementary Materials: The following supporting information can be downloaded at: <https://www.mdpi.com/article/10.3390/molecules29102378/s1>, Figure S1: IR spectrum of **Ag[Cl}_6\text{-1}**; Figure S2: IR spectrum of **5**; Figure S3: (a) $^1\text{H}\{^{11}\text{B}\}$ -NMR and (b) $^{11}\text{B}\{^1\text{H}\}$ -NMR spectra of **Ag[Cl}_6\text{-1}** compound in acetone-*d*₆; Figure S4: (a) ^1H -NMR; (b) $^1\text{H}\{^{11}\text{B}\}$ -NMR; (c) $^{11}\text{B}\{^1\text{H}\}$ -NMR (d) ^{11}B -NMR and (e) COSY NMR spectra of **5**. compound in acetone-*d*₆; Figure S5: UV-visible of **Ag[Cl}_6\text{-1}** compound in CH_2Cl_2 ; Figure S6: CV of (a) **Ag[Cl}_6\text{-1}** compound in $\text{CH}_3\text{CN} + 0.1 \text{ M TBAH}$ vs. Ag/AgCl ; (b) **5** in $\text{CH}_3\text{CN} + 0.1 \text{ M TBAH}$ vs. Ag/AgCl ; and (c) **5** in a phosphate buffer (pH = 7.12) vs. Ag/AgCl ; scan rate $V = 100 \text{ mV/s}$; Figure S7: Plot of conversion as a function of time for the photoredox catalysis of styrene. Conditions: **4** (0.01 mM), styrene (20 mM), $\text{Na}_2\text{S}_2\text{O}_8$ (26 mM), 5 mL aqueous solution at pH = 7, light irradiation (2.2 W, $\lambda \sim 300 \text{ nm}$); Figure S8: ESI-MS spectra of **5**; Table S1: Photooxidation tests performed with complex **4**. Conditions: **4** (0.01 mM), substrate (20 mM), $\text{Na}_2\text{S}_2\text{O}_8$ (26 mM), 5 mL aqueous solution at pH = 7; Table S2: Photooxidation of epoxides performed with complex **4**. Conditions: **4** (0.01 mM), epoxide (20 mM), $\text{Na}_2\text{S}_2\text{O}_8$ (26 mM), 5 mL aqueous solution at pH = 7; Table S3: Photooxidation tests performed with **5** complex. Conditions: **5** (0.001 mM), substrate (20 mM), $\text{Na}_2\text{S}_2\text{O}_8$ (26 mM), 5 mL aqueous solution at pH = 7.

Author Contributions: Conceptualization, F.T. and I.R.; methodology, I.G., F.T. and I.R.; writing—original draft preparation, I.G. and I.R.; writing—review and editing, I.G., C.V., F.T. and I.R.; supervision, F.T. and I.R.; project administration, F.T. and I.R.; funding acquisition, F.T., C.V. and I.R. All authors have read and agreed to the published version of the manuscript.

Funding: This work was financially supported by AGAUR (Generalitat de Catalunya, project 2021-SGR-00442), MICINN (PID2019-106832RB-I00, PID2022-136892NB-I00), and the Severo Ochoa Program for Centers of Excellence for the FUNFUTURE CEX2019-000917-S project).

Institutional Review Board Statement: Not applicable.

Informed Consent Statement: Not applicable.

Data Availability Statement: Data are contained within the article and supplementary materials.

Conflicts of Interest: The authors declare no conflicts of interest.

References

1. Gagnon, S.D.H.F. *Encyclopedia of Polymer Science and Engineering*, 2nd ed.; Mark, H.F., Bikales, N.M., Overberger, C.G., Menges, G., Kroschwitz, J.I., Eds.; John Wiley & Sons: New York, NY, USA, 1985; Volume 6, pp. 273–307.
2. de Faveri, G.; Ilyashenko, G.; Watkinson, M. Recent advances in catalytic asymmetric epoxidation using the environmentally benign oxidant hydrogen peroxide and its derivatives. *Chem. Soc. Rev.* **2011**, *40*, 1722–1760. [[CrossRef](#)]
3. Smith, J.G. Synthetically useful reactions of epoxides. *Synthesis* **1984**, *1984*, 629–656. [[CrossRef](#)]
4. Jacobsen, E.N. Asymmetric catalysis of epoxide ring-opening reactions. *Accounts Chem. Res.* **2000**, *33*, 421–431. [[CrossRef](#)] [[PubMed](#)]
5. de Vries, E.J.; Janssen, D.B. Biocatalytic conversion of epoxides. *Curr. Opin. Biotechnol.* **2003**, *14*, 414–420. [[CrossRef](#)] [[PubMed](#)]
6. Muzart, J. Pd-Mediated Reactions of Epoxides. *Eur. J. Org. Chem.* **2011**, *25*, 4717–4741. [[CrossRef](#)]
7. Jacobsen, E.N.; Zhang, W.; Muci, A.R.; Ecker, J.R.; Deng, L. Highly enantioselective epoxidation catalysts derived from 1,2-diaminocyclohexane. *J. Am. Chem. Soc.* **1991**, *113*, 7063–7064. [[CrossRef](#)]
8. Cussó, O.; Garcia-Bosch, I.; Ribas, X.; Lloret-Fillol, J.; Costas, M. Asymmetric epoxidation with H₂O₂ by manipulating the electronic properties of non-heme iron catalysts. *J. Am. Chem. Soc.* **2013**, *135*, 14871–14878. [[CrossRef](#)]
9. Jeon, S.-J.; Li, H.; Walsh, P.J. A green chemistry approach to a more efficient asymmetric catalyst: Solvent-free and highly concentrated alkyl additions to ketones. *J. Am. Chem. Soc.* **2005**, *127*, 16416–16425. [[CrossRef](#)] [[PubMed](#)]
10. Sartori, S.K.; Miranda, I.L.; Diaz, M.A.N.; Diaz-Munoz, G. Sharpless asymmetric epoxidation: Applications in the synthesis of bioactive natural products. *Mini Rev. Org. Chem.* **2021**, *18*, 606–620. [[CrossRef](#)]
11. Serrano, I.; López, M.I.; Ferrer, I.; Poater, A.; Parella, T.; Fontrodona, X.; Solà, M.; Llobet, A.; Rodríguez, M.; Romero, I. New Ru (II) complexes containing oxazoline ligands as epoxidation catalysts. Influence of the substituents on the catalytic performance. *Inorg. Chem.* **2011**, *50*, 6044–6054. [[CrossRef](#)]
12. Ferrer, I.; Fontrodona, X.; Roig, A.; Rodríguez, M.; Romero, I. A recoverable ruthenium aqua complex supported on silica particles: An efficient epoxidation catalyst. *Chem. Eur. J.* **2017**, *23*, 4096–4107. [[CrossRef](#)]
13. Ye, D.; Liu, L.; Peng, Q.; Qiu, J.; Gong, H.; Liu, S. Effect of Controlling Thiophene Rings on D-A Polymer Photocatalysts Accessed via Direct Arylation for Hydrogen Production. *Molecules* **2023**, *28*, 4507. [[CrossRef](#)]
14. Lang, X.; Zhao, J.; Chen, X. Cooperative photoredox catalysis. *Chem. Soc. Rev.* **2016**, *45*, 3026–3038. [[CrossRef](#)] [[PubMed](#)]
15. Glasser, F.; Wenger, O.S. Recent progress in the development of transition-metal based photoredox catalysts. *Coord. Chem. Rev.* **2020**, *405*, 213129. [[CrossRef](#)]
16. Clerich, E.; Affès, S.; Anticó, E.; Fontrodona, X.; Teixidor, F.; Romero, I. Molecular and supported ruthenium complexes as photoredox oxidation catalysts in water. *Inorg. Chem. Front.* **2022**, *9*, 5347–5359. [[CrossRef](#)]
17. Affès, S.; Stamatelou, A.-M.; Fontrodona, X.; Kabadou, A.; Viñas, C.; Teixidor, F.; Romero, I. Enhancing Photoredox Catalysis in Aqueous Environments: Ruthenium Aqua Complex Derivatization of Graphene Oxide and Graphite Rods for Efficient Visible-Light-Driven Hybrid Catalysts. *ACS Appl. Mater. Interfaces* **2024**, *16*, 507–519. [[CrossRef](#)]
18. Chen, W.; Rein, F.N.; Scott, B.L.; Rocha, R.C. Catalytic Photooxidation of Alcohols by an Unsymmetrical Tetra (pyridyl) pyrazine-Bridged Dinuclear Ru Complex. *Chem. Eur. J.* **2011**, *17*, 5595–5604. [[CrossRef](#)] [[PubMed](#)]
19. Lennox, A.J.J.; Fischer, S.; Jurrat, M.; Luo, S.P.; Rockstroh, N.; Junge, H.; Ludwig, R.; Beller, M. Copper-Based Photosensitisers in Water Reduction: A More Efficient In Situ Formed System and Improved Mechanistic Understanding. *Chem. Eur. J.* **2016**, *22*, 1233–1238. [[CrossRef](#)] [[PubMed](#)]
20. Farràs, P.; Maji, S.; Benet-Buchholz, J.; Llobet, A. Synthesis, Characterization, and Reactivity of Dyad Ruthenium-Based Molecules for Light-Driven Oxidation Catalysis. *Chem. Eur. J.* **2013**, *19*, 7162–7172. [[CrossRef](#)]
21. Hockin, B.M.; Li, C.; Robertson, N.; Zysman-Colman, E. Photoredox catalysts based on earth-abundant metal complexes. *Catal. Sci. Technol.* **2019**, *9*, 889–915. [[CrossRef](#)]
22. Fukuzumi, S.; Kishi, T.; Kotani, H.; Lee, Y.M.; Nam, W. Highly efficient photocatalytic oxygenation reactions using water as an oxygen source. *Nat. Chem.* **2011**, *3*, 38–41. [[CrossRef](#)] [[PubMed](#)]
23. Chen, G.; Chen, L.; Ma, L.; Kwonga, H.-K.; Lau, T.-C. Photocatalytic oxidation of alkenes and alcohols in water by a manganese (v) nitrido complex. *Chem. Commun.* **2016**, *52*, 9271–9274. [[CrossRef](#)] [[PubMed](#)]
24. Guerrero, I.; Viñas, C.; Romero, I.; Teixidor, F. A stand-alone cobalt bis(dicarbollide) photoredox catalyst epoxidates alkenes in water at extremely low catalyst load. *Green Chem.* **2021**, *23*, 10123–10131. [[CrossRef](#)]
25. Fontanet, M.; Rodríguez, M.; Vinas, C.; Teixidor, F.; Romero, I. Carboranycarboxylate complexes as efficient catalysts in epoxidation reactions. *Eur. J. Inorg. Chem.* **2017**, *2017*, 4425–4429. [[CrossRef](#)]
26. Mukherjee, S.; Thilagar, P. Boron clusters in luminescent materials. *Chem. Commun.* **2016**, *52*, 1070–1093. [[CrossRef](#)] [[PubMed](#)]

27. Junki, O.; Kazuo, T.; Yoshiki, T. Recent progress in the development of solid-state luminescent o-carboranes with stimuli responsivity. *Angew. Chem. Int. Ed.* **2020**, *59*, 9841–9855.
28. Shi, C.; Sun, H.; Jiang, Q.; Zhao, Q.; Wang, J.; Huang, W.; Yan, H. Carborane tuning of photophysical properties of phosphorescent iridium(III) complexes. *Chem. Commun.* **2013**, *49*, 4746–4748. [[CrossRef](#)] [[PubMed](#)]
29. Hawthorne, M.F.; Young, D.C.; Garret, P.M.; Owen, D.A.; Schwerin, S.G.; Tebbe, F.N.; Wegner, P.M. Preparation and characterization of the (3)-1,2-and (3)-1,7-dicarbododecahydroundecaborate (−1) ions. *J. Am. Chem. Soc.* **1968**, *90*, 862–868. [[CrossRef](#)]
30. Bennour, I.; Cioran, A.M.; Teixidor, F.; Viñas, C. 3, 2, 1 and stop! An innovative, straightforward and clean route for the flash synthesis of metallacarboranes. *Green Chem.* **2019**, *21*, 1925–1928. [[CrossRef](#)]
31. Fuentes, I.; Andrio, A.; Teixidor, F.; Viñas, C.; Compan, V. Enhanced conductivity of sodium versus lithium salts measured by impedance spectroscopy. Sodium cobaltacarboranes as electrolytes of choice. *Phys. Chem. Chem. Phys.* **2017**, *19*, 15177–15186. [[CrossRef](#)]
32. Stoica, A.-I.; Viñas, C.; Teixidor, F. Cobaltabisdicarbollide anion receptor for enantiomer-selective membrane electrodes. *Chem. Commun.* **2009**, 4988–4990. [[CrossRef](#)] [[PubMed](#)]
33. Fuentes, I.; Pujols, J.; Viñas, C.; Ventura, S.; Teixidor, F. Dual binding mode of metallacarborane produces a robust shield on proteins. *Chem. Eur. J.* **2019**, *25*, 12820–12829. [[CrossRef](#)] [[PubMed](#)]
34. Pazderová, L.; Tüzün, E.Z.; Bovol, D.; Litecká, M.; Fojt, L.; Grüner, B. Chemistry of Carbon-Substituted Derivatives of Cobalt Bis(dicarbollide)(1[−]) Ion and Recent Progress in Boron Substitution. *Molecules* **2023**, *28*, 6971. [[CrossRef](#)] [[PubMed](#)]
35. Bauduin, P.; Prevost, S.; Farràs, P.; Teixidor, F.; Diat, O.; Zemb, T. A theta-shaped amphiphilic cobaltabisdicarbollide anion: Transition from monolayer vesicles to micelles. *Angew. Chem. Int. Ed.* **2011**, *50*, 5298–5300. [[CrossRef](#)] [[PubMed](#)]
36. Uchman, M.; Ďord'ovič, V.; Tošner, Z.; Matějček, P. Classical amphiphilic behavior of nonclassical amphiphiles: A comparison of metallacarborane self-assembly with SDS micellization. *Angew. Chem. Int. Ed.* **2015**, *54*, 14113–14117. [[CrossRef](#)] [[PubMed](#)]
37. Zaulet, A.; Teixidor, F.; Bauduin, P.; Diat, O.; Hirva, P.; Ofori, A.; Viñas, C. Deciphering the role of the cation in anionic cobaltabisdicarbollide clusters. *J. Organomet. Chem.* **2018**, *865*, 214–225. [[CrossRef](#)]
38. Guerrero, I.; Kelemen, Z.; Viñas, C.; Romero, I.; Teixidor, F. Metallacarboranes as photoredox catalysts in water. *Chem. Eur. J.* **2020**, *26*, 5027–5036. [[CrossRef](#)] [[PubMed](#)]
39. Guerrero, I.; Saha, A.; Xavier, J.A.M.; Viñas, C.; Romero, I.; Teixidor, F. Noncovalently linked metallacarboranes on functionalized magnetic nanoparticles as highly efficient, robust, and reusable photocatalysts in aqueous medium. *ACS Appl. Mater. Interfaces* **2020**, *12*, 56372–56384. [[CrossRef](#)] [[PubMed](#)]
40. Guerrero, I.; Fontrodona, X.; Viñas, C.; Romero, I.; Teixidor, F. Aqueous persistent noncovalent ion-pair cooperative coupling in a ruthenium cobaltabis (dicarbollide) system as a highly efficient photoredox oxidation catalyst. *Inorg. Chem.* **2021**, *60*, 8898–8907. [[CrossRef](#)]
41. Rodríguez, M.; Romero, I.; Sens, C.; Llobet, A. Ru=O complexes as catalysts for oxidative transformations, including the oxidation of water to molecular dioxygen. *J. Mol. Catal. A Chem.* **2006**, *251*, 215–220. [[CrossRef](#)]
42. Takeuchi, K.J.; Tompson, M.S.; Pipes, D.V.; Meyer, T.J. Redox and spectral properties of monooxo polypyridyl complexes of ruthenium and osmium in aqueous media. *Inorg. Chem.* **1984**, *23*, 1845–1851. [[CrossRef](#)]
43. Mátel, L.; Macášek, F.; Rajec, P.; Heřmánek, S.; Plešek, J. B-Halogen derivatives of the bis (1,2-dicarbollyl) cobalt (III) anion. *Polyhedron* **1982**, *1*, 511–519. [[CrossRef](#)]
44. Rojo, I.; Teixidor, F.; Viñas, C.; Kivekäs, R.; Sillanpää, R. Relevance of the electronegativity of boron in η⁵-coordinating ligands: Regioselective monoalkylation and monoarylation in cobaltabisdicarbollide [3,3'-Co(1,2-C₂B₉H₁₁)₂][−] clusters. *Chem. Eur. J.* **2003**, *9*, 4311–4323. [[CrossRef](#)] [[PubMed](#)]
45. Cerný, V.; Pavlík, J.; Kustková-Maxová, E. Ligand field theory, d-d spectra of ferrocene and other d⁶-metallocenes. *Collect. Czechoslov. Chem. Commun.* **1976**, *41*, 3232–3244. [[CrossRef](#)]
46. Balzani, V.; Juris, M.; Campagna, S.; Serroni, S. Luminescent and redox-active polynuclear transition metal complexes. *Chem. Rev.* **1996**, *96*, 759–834. [[CrossRef](#)] [[PubMed](#)]
47. Moyer, B.A.; Thompson, M.S.; Meyer, T.J. Chemically catalyzed net electrochemical oxidation of alcohols, aldehydes, and unsaturated hydrocarbons using the system (trpy)(bpy)Ru(OH)₂²⁺ / (trpy)(bpy)RuO²⁺. *J. Am. Chem. Soc.* **1980**, *102*, 2310–2312. [[CrossRef](#)]
48. Behr, A.; Westfachtel, A.; Pérez Gomes, J. Catalytic processes for the technical use of natural fats and oils. *Chem. Eng. Technol.* **2008**, *31*, 700–714. [[CrossRef](#)]
49. Sullivan, B.P.; Calvert, J.M.; Meyer, T.J. Cis-trans isomerism in (trpy)(PPh₃)RuCl₂. Comparisons between the chemical and physical properties of a cis-trans isomeric pair. *Inorg. Chem.* **1980**, *19*, 1404–1407. [[CrossRef](#)]

Disclaimer/Publisher's Note: The statements, opinions and data contained in all publications are solely those of the individual author(s) and contributor(s) and not of MDPI and/or the editor(s). MDPI and/or the editor(s) disclaim responsibility for any injury to people or property resulting from any ideas, methods, instructions or products referred to in the content.